

Effect of Deposition Layer of Titanium Dioxide (TiO₂) Thin Film as Photoanode For Economically Sustainable Dye-Sensitized Solar Cell (DSSC) Application

Nur Alfarina Pirdaus^{1,2}, Irfan Nazif Nordin Amini², Wan Abd Al Qadr Imad Wan Mohtar³, Muhammad Azfar Shamil Abd Aziz¹, Nurfadzilah Ahmad^{1,2}

¹Solar Research Institute (SRI), Universiti Teknologi MARA (UiTM) Shah Alam, Selangor, ²School of Electrical Engineering, College of Engineering, Universiti Teknologi MARA (UiTM) Shah Alam, Selangor, ³Functional Omics and Bioprocess Development Laboratory, Institute of Biological Sciences, Faculty of Science, Universiti Malaya, 50603 Kuala Lumpur, Malaysia
Correspondence Author Email: nurfadzilah6344@uitm.edu.my

To Link this Article: <http://dx.doi.org/10.6007/IJAREMS/v12-i3/19238> DOI:10.6007/IJAREMS/v12-i3/19238

Published Online: 28 September, 2023

Abstract

For decades, silicon solar cells had been established as commercialized solar cell. However, silicon solar cells require high cost and tedious fabrication techniques that utilized chemical which may be toxic to the environment. In this case, dye-sensitized solar cell (DSSC) has gained recognition in these recent years due to its simple and low-cost fabrication technique by utilizing natural resources when compared to commercial silicon solar cells which are fully chemical-based synthesis. DSSC is a thin film solar cell typically consist of a thin layer of porous titanium dioxide (TiO₂) coated on a transparent conductive oxide such as indium tin oxide (ITO) or fluorine-doped tin oxide (FTO), light-absorbing dye, counter electrode and electrolyte to regenerate the electron. In this study, the effects of TiO₂ thin film thickness were analyzed to determine whether the thickness of TiO₂ thin film has significant effect on the performance of the DSSC device. TiO₂ in this study was synthesized using sol-gel method with titanium (IV) butoxide used as the precursor. Spin coating method was utilized to deposit the thin film layers. Analysis on the structural, morphology, optical and electrical properties of the TiO₂ thin film using X-ray Diffraction (XRD), Field Emission Scanning Electron Microscopy (FESEM), Ultraviolet-visible Spectrophotometry (UV-Vis) and 2-Point Probe respectively. The results for XRD pattern identified the production of the amorphous phase of TiO₂ structured thin films, with a tendency towards anatase phase at 25° (highest peak on 3 deposition layers). FESEM images demonstrate that the TiO₂ thin film with 3 layers has more porous, agglomerated, and compact morphology than the other two deposition layers. The bandgap energy of TiO₂ thin films calculated from Tauc plot based on UV-visible absorbance spectra were 2.24 eV, 2.13 eV, and 2.04 eV for 1, 2, and 3 deposition layers, respectively. These properties indicate that

3 deposition layers is the optimized deposition layer of TiO₂ thin film for DSSC application which will ensure good absorption of dye molecules onto the semiconducting metal oxide layer. Further research and new findings on other components like dye, electrolyte and counter electrode also necessary to improve the efficiency and stability of DSSC for future commercialization potential which will be more economically sustainable.

Keywords: Solar Cell, DSSC, Titanium Dioxide, Sol-Gel, Deposition Layer

Introduction

Photovoltaics (PV) is a process of utilising semiconducting materials that exhibit the photovoltaic effect to collect solar light and convert them into energy. Photovoltaic cell or solar cell utilising the photovoltaic effect is a method which directly convert light energy into electricity [1].

Dye-sensitized solar cells, a type of third generation solar cell is gaining interest in photovoltaic technology because of their potential to convert energy at a low cost [2]. O'Regan and Gratzel developed the dye-sensitized solar cells (DSSC) in 1991. DSSC have garnered a lot of interest because of their performance, low production costs, lower weight and low toxicity [3]. These type of solar cell are more effective than other thin films, yet are still less efficient than crystalline solar cells [4].

The photoanodes for the older generation of solar cells were typically made of semiconductor materials like CdS, Si, or GaAs, but eventually they became electrochemically unstable in response to photo-corrosion when exposed to light. Large bandgap (approximately 3 eV) semiconductors such ZnO, TiO₂, and SnO₂ commonly utilised in the fabrication of DSSC provide a chemically stable cell since they are resistant to photo-corrosion [5].

The photoanode, which is made of semiconducting oxide materials like (TiO₂, ZnO, etc.), as well as organic or inorganic dye molecules that act as sensitizers, iodide/tri-iodide-based electrolytes that act as redox mediators, and counter electrodes made of platinum or carbon are the main components of DSSC. The excited electrons from the dye molecules are injected into TiO₂'s conduction band during photon absorption from sunlight and diffuse through the transparent conductive oxide (TCO) to the external circuit [6].

Among the those semiconducting metal oxide nanomaterials, titanium dioxide (TiO₂) is a material of interest for various applications due to its non-toxic nature, good optical electrical capabilities and great stability in DSSC and other photocatalytic applications. Anatase phase of TiO₂ is used as a photoanode in DSSC and as a photocatalyst for organic molecule degradation because it is an effective charge separator of photoexcited charge carriers. The quantity of dye molecules adsorbed on TiO₂ surfaces, the number of photons absorbed by the dye molecules for effective electron harvesting and the number of electron-hole pair recombinations are the main factors influencing the effectiveness of DSSC and photocatalytic applications. For enhancing TiO₂ absorption into the visible region, researchers have employed a variety of strategies [7].

Numerous methods have been used to produce TiO₂ nanoparticles. Geffcken and Berger first introduced the sol-gel process in 1939 and it has attracted a lot of interest since then. On account of its basic operation, low reaction temperature, great chemical homogeneity, simple substrate requirements and high product purity, it has become a common technique for generating TiO₂ [2]. The sol-gel method is one of the most common synthesis techniques to generate nanomaterials since it involves only ambient temperature and pressure for the synthesis process, requiring no extensive preparations. In

sol-gel synthesis, a titanium precursor is hydrolysed or condensed to yield a sol and then a gel. A xerogel is created immediately after the solvent evaporates and it is ground and heated to produce crystalline TiO₂ nanopowders [8].

To increase the amount of light that was potentially absorbed, a nanoporous TiO₂ electrode with a large surface area per projected area was used [9]. Rutile, anatase, and brookite are the three polymorphisms of TiO₂. The three structures are metastable, with rutile structure being the most thermodynamically stable. Comparing to TiO₂ from the rutile phase, which has a band gap of 3.0 eV, anatase phase TiO₂ has a wider energy band gap of 3.2 eV, improving photoactivity and making it the most suitable choice for DSSC applications [10].

Most of mesoporous TiO₂ nanoparticles used in DSSC fabrication have surface areas between 50 and 250 m²/g. The conducting side of TCO glass is coated with TiO₂. The most preferred TiO₂ coating methods including screen printing, doctor blade method, spin coating, electrophoretic deposition and tape casting. After removing organic binders and obtaining a pure TiO₂ film, a high temperature heat treatment is used to improve the inter-particle adhesion of the TiO₂ nanoparticles [5]. Align with the aim of this paper to investigate impact of TiO₂ thin film thickness for DSSC application [2].

Methodology

A. *Preparation Of TiO₂ Nanoparticles by Sol-Gel Method*

All of the chemical substances are in analytical grade and have not undergone further processing. The TiO₂ was made by mixing 50 ml of titanium (IV) butoxide with 50 ml of ethanol and stirred for an hour. The solution was then gradually diluted with 25 ml of deionized water after that. The resulting gel formed almost immediately and was stirred again for few minutes. The solution was filtered after kept for 24 hours. The leftover water and organic material will then be evaporated for the following 12 hours in a 100°C oven. The substance was milled into a fine powder after drying.

B. *Preparation Of TiO₂-Coated Thin Film*

2 g of the prepared TiO₂ powder was added into 100 ml of ethyl alcohol and stirred for 30 minutes to form a homogenous TiO₂ paste. Before usage, the solution was kept in the dark.

The glass substrate was cleaned in a sonicator for 15 minutes alternately with ethanol and deionized water before coating. 10 drops of TiO₂ paste were dropped onto the dried and cleaned glass substrates at a speed of 3000 rpm to create a single layer of coating. The glass substrate was then dried at 100°C for 10 minutes. The same technique was repeated for second and third layer of coating. The final coating underwent a 30-minute annealing at 500°C.

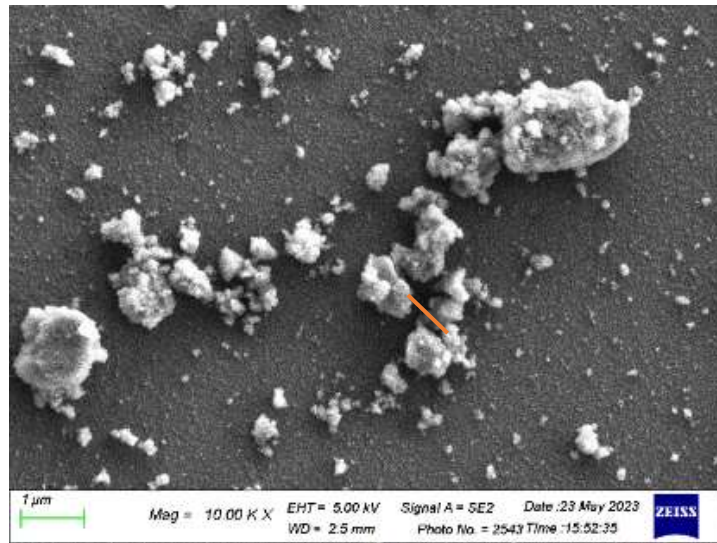
C. *Characterisation*

FESEM was utilised for analysing the surface morphology of the TiO₂ while UV-Visible spectrometer was used to evaluate the transmittance and bandgap energy of both types of TiO₂ at the 300 nm to 800 nm range. X-ray diffraction (XRD) was used to identify the phase of the thin film spin coated with different layers and 2-point probe was used to measure the current-voltage for electrical properties analysis.

Results and Discussion

A. Morphological analysis

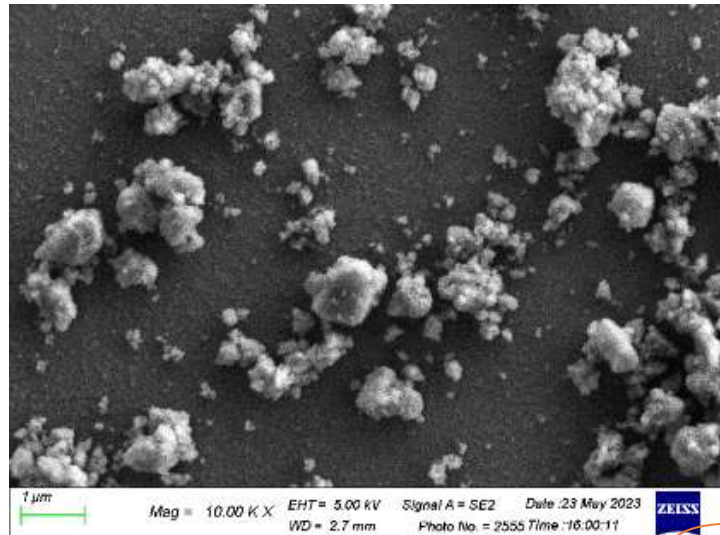
FESEM images in Fig. 1, Fig. 2 and Fig. 3 show the microstructure of 3 deposition layers of TiO₂ thin films in 10K magnification.



Results

File	Edit	Font	Results				
	Label	Area	Mean	Min	Max	Angle	Length
1		0.008	219.155	65.000	254.000	-86.583	0.738
2		0.004	196.409	119.000	248.133	25.769	0.354
3		0.004	196.409	119.000	248.133	25.769	0.354
4		0.004	215.842	128.000	254.000	32.347	0.390
5		0.004	191.545	56.000	251.000	-90.000	0.352
6		0.006	153.562	51.493	233.129	129.369	0.554
7		0.005	198.292	77.000	245.444	-130.601	0.405
8		0.005	207.044	83.000	254.000	-43.091	0.466
9		0.004	199.068	150.000	253.008	-75.964	0.362
10		0.006	155.755	49.859	230.708	-79.160	0.526
11	Mean	0.005	193.308	89.835	247.156	-29.214	0.450
12	SD	0.001	22.198	36.238	8.574	79.668	0.125
13	Min	0.004	153.562	49.859	230.708	-130.601	0.352
14	Max	0.008	219.155	150.000	254.000	129.369	0.738

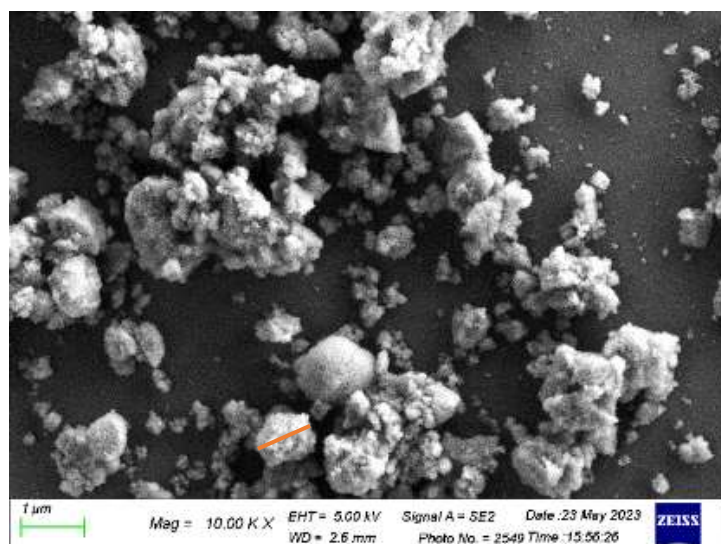
Fig. 1. FESEM images of 1 deposition layer of TiO₂ thin film (10,000x magnification, bar = 1μm, 1 μm = 1000 nm).



Results

File	Edit	Font	Results				
	Label	Area	Mean	Min	Max	Angle	Length
1		0.005	163.777	53.000	242.364	-87.397	0.481
2		0.008	103.282	61.450	181.317	-27.378	0.689
3		0.004	147.709	52.000	213.569	-103.134	0.337
4		0.004	140.894	55.000	190.944	-57.381	0.324
5		0.005	159.906	58.000	223.010	-79.824	0.433
6		0.007	148.775	57.000	242.041	42.825	0.611
7		0.008	113.920	34.312	198.330	50.194	0.683
8		0.006	83.545	53.000	122.767	-66.161	0.514
9		0.004	119.670	61.776	178.579	-78.690	0.334
10		0.006	194.709	105.255	250.643	-37.304	0.577
11	Mean	0.006	137.619	59.079	204.356	-44.425	0.498
12	SD	0.002	32.768	17.965	38.742	52.986	0.140
13	Min	0.004	83.545	34.312	122.767	-103.134	0.324
14	Max	0.008	194.709	105.255	250.643	50.194	0.689

Fig. 2. FESEM images of 2 deposition layers of TiO₂ thin film. (10,000x magnification, bar = 1μm, 1 μm = 1000 nm)



Results

File Edit Font Results							
	Label	Area	Mean	Min	Max	Angle	Length
1		0.008	118.681	25.000	198.420	3.318	0.754
2		0.006	129.415	71.000	196.606	-65.925	0.562
3		0.008	200.263	80.000	254.000	-88.363	0.764
4		0.012	120.318	41.000	205.215	-25.320	1.122
5		0.007	105.786	48.000	186.393	-68.009	0.612
6		0.005	119.471	32.000	204.500	-94.289	0.438
7		0.007	132.648	25.000	235.579	-82.999	0.626
8		0.006	146.438	88.087	222.217	-7.431	0.506
9		0.006	157.878	70.000	239.000	-90.000	0.524
10		0.004	125.589	58.000	199.248	39.806	0.341
11		0.004	77.005	32.000	118.000	-9.462	0.398
12	Mean	0.007	130.317	51.826	205.380	-44.425	0.604
13	SD	0.002	31.205	22.808	35.846	46.185	0.218
14	Min	0.004	77.005	25.000	118.000	-94.289	0.341
15	Max	0.012	200.263	88.087	254.000	39.806	1.122

Fig. 3. FESEM images of 3 deposition layers of TiO₂ thin film. (10,000x magnification, bar = 1 μm, 1 μm = 1000 nm)

From the FESEM images, it can be seen that thin film with 3 deposition layers (Fig. 3) which is the thickest layer, appeared to be in highly compact with a widespread sand-like particles which is highly agglomerated with irregular structure of particles compared to 1 and 2 deposition layers.

The average particle size of 1 layer TiO₂ thin film deposition was 450 nm (see Fig. 1). TiO₂ attained a mean particle size of 498 nm for 2 layers of deposition (see Fig. 2) while TiO₂ thin film deposited in 3 layers have the measured mean particle size of 604 nm (see Fig. 3). It can be deduced that as the thickness of the TiO₂ deposition layer increase, the particle size increases. Addition of TiO₂ layers in the form of nanoparticles will improve the performance of solar cells fabricated by ensuring the electron injection [11].

Agglomeration and aggregation of the irregular sized particle are primarily caused by the high surface energy of the materials, leading them to clump and cluster in order to reduce their surface energies [12]. Weak photon diffusion towards the inner region of the TiO₂ layer is caused by increasing TiO₂ particle sizes. This reduces the number of photogenerated carriers, which has a small impact on the photocurrent. Furthermore, the rate of electron-hole pair recombination is accelerated by higher particle sizes. More electrons and holes recombining leads to a significant decrease in the amount of charge carriers, which reduces photocurrent detection [13]. In order to be deposited on a transparent conductive oxide (TCO) substrate, TiO₂ paste should have the nanoparticles size with no larger than 20 nm [14].

Findings revealed that different thickness of deposition layer improve the dilution of electrolyte species surround the TiO₂ film while smaller surface area reduces the time needed for electrons to travel through the film [15]. Wide surface area and porous structure of photoanode increase the light absorption of the thin film. DSSC efficiency increase with increase in TiO₂ film thickness because the condition will provide better dye absorption capacity. However, longer route length for electron transport will increase the recombination of photo-excited electrons with I³ ions at the surface of TiO₂, thus reduced transparency of TiO₂ thin film. This condition will reduce conversion efficiency [16]. The TiO₂ film layer adsorbent properties and absorption performance will depend on the film thickness and compactness after being immersed in dye [17].

B. Structural Analysis

Structural properties of TiO₂ thin films with different layers of deposition were studied using X-ray Diffraction (XRD) analysis ranging the 2theta of 10° to 90°. The XRD pattern in Fig. 4 can be observed not showing a clear peak of crystallisation. This condition indicating the presence of amorphous phase. However, the peak was not totally absent, a potential peak of anatase still can be seen at 25°. From literature, anatase is the preferred orientation. The orientation of this phase is in (101), (004), (210), (200), (111), (211) planes at 25.35°, 37.56°, 41.45°, 44.48°, 45.45°, 55.72° peaks which aligned with JCPDS data [13] [18]. Anatase has been proven to perform as an indirect semiconductor which exhibit electron excitation from the conduction band to the valence band. Anatase also has a longer electron-hole lifetime than rutile which is a direct semiconductor with a lower carrier lifetime [19].

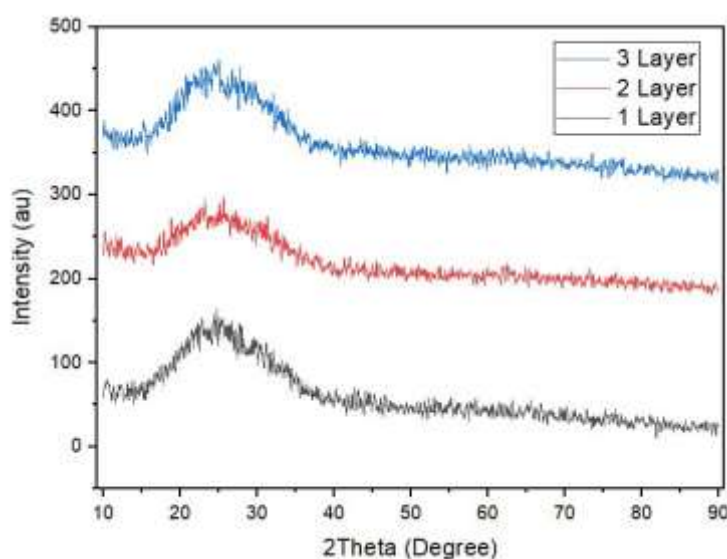


Fig. 4. XRD spectra of 3 deposition layers of TiO₂ thin films.

When the film thickness was increased, the peaks of the (101)-plane for the samples sharpened, indicating the enhancement of crystallinity. The (101) peaks of TiO₂ films displayed a clear alignment of the (101)-axis with the substrate surface. These results demonstrate that TiO₂ film structure is improved by increasing film thickness [20].

Considering anatase has a more flexible molecular structure than rutile, the initial phase development of crystalline TiO₂ synthesis is often anatase, thereby the short-range order of TiO₆ octahedra can be easily assembled into long-range anatase structure. In other words, anatase is the preferred phase generated during TiO₂ synthesis due to their more flexible structure which leads to enhanced formation kinetics [21].

Theoretically, sol-gel precipitates produced by the sol gel process are typically amorphous. Thus, further heat treatment required for crystallisation to occur. Annealing temperature higher than 300°C is usually required to initiate the transition from amorphous to anatase phase, triggering a significant increase in particle size [22]. In this case, impurities from the sample preparation have to be avoided to prevent a reduction in the intensity of desired diffraction peaks.

TiO₂ suggests that a 400°C heat treatment might convert the rutile phase into the anatase phase, in accordance with prior studies [5]. In contrast, all of the samples in this experiment remained in amorphous condition even after being annealed at 500°C for 30 minutes, but they were almost in the anatase phase. The results of this experiment may have been affected by the pH value and annealing time utilised, according to further research.

C. Optical analysis

From Fig. 5 below, TiO₂ thin films with three different deposition layers without the addition of dyes coating in wavelength range between 300 and 800 nm were observed according to the transmittance and band gap energy.

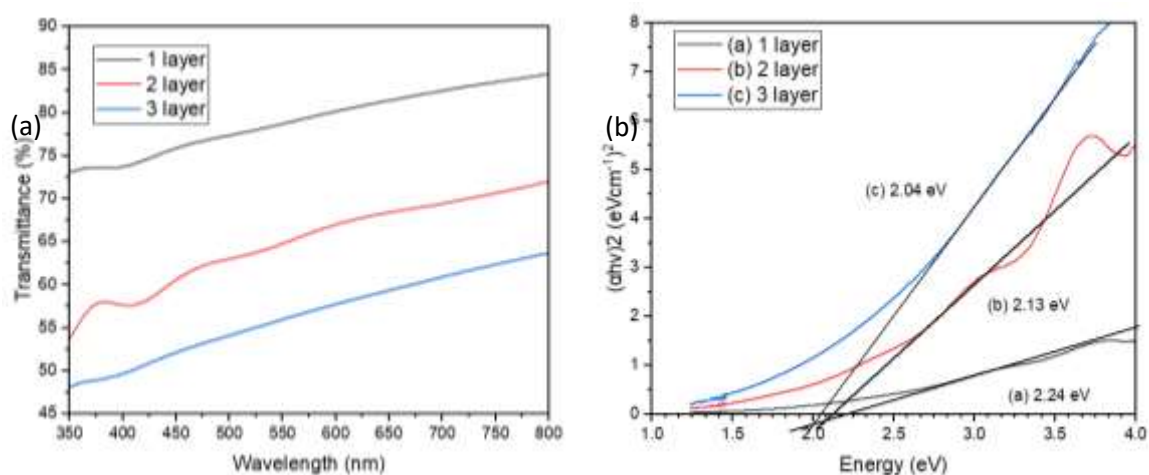


Fig. 5. (a) Transmittance spectra and (b) Tauc plots of 3 different deposition layers of TiO₂ thin films.

The optical transmittance measurements for TiO₂ thin film samples are shown in Fig. 5 (a). The transmittance for all 3 samples shown the increasing transmittance. All 3 samples exhibited small increase in transmittance. However, 1 deposition layer thin film exhibited highest transmittance which maximum at 85%. Comparing the 3 different deposition layers thin films, it can be seen that transmittance values decrease as film thickness increases. The decrease in transmittance with increasing film thickness is related to the free carrier absorption and photon scattering because of the rougher surface of the film [23].

Beer's law was used to estimate the optical band gap energy (E_g) based on the absorbance spectra obtained from UV-Vis characterization and Tauc plot was used to calculate the E_g using the following equation:

$$\alpha h\nu = A(h\nu - E_g)^n \quad (1)$$

where α is the absorption coefficient, E_g is the nanoparticle band gap value, $h\nu$ is energy of photon and A is the constant associated with the effective masses of the bonds, n denotes the transition nature; $n = 2$ corresponding to the allowed indirect transitions. It was estimated by extrapolating the linear portion of $(\alpha h\nu)^2$ vs photon energy curve to the photon energy axis respectively [24].

The tauc plot of TiO₂ thin films produced at various deposition layers is shown in Fig. 5 (b). While the thin films with thicker layers of 2 and 3 layers recorded band gap energy values of 2.13 eV and 2.04 eV respectively, TiO₂ thin film with 1 layer displays larger energy band gap with value of 2.24 eV.

The optical bandgap values decrease with increasing film thickness, which is due to the addition of new energy levels near the valence band inside the energy gap brought about by the increase in film thickness. This condition creates bridges for the electrons (with lower energies than the energy gap value for the first thin film) transmitted between the valence band and the conduction band, increasing the quantity of electron transfers and altering the Fermi level. Due to reaching the lowest bandgap energy in this instance, 3 layers TiO₂ deposition layers thin film shows the largest number of electrons that can be transferred [11].

D. Electrical analysis

The current-voltage (I-V) measurements of sol-gel synthesised TiO₂ thin films for different deposition layers are shown in Fig. 5. Due to its symmetrical and linear shape, it implies that the TiO₂ thin film and the Au metal contact possess ohmic contact characteristics [25]. The thicker deposition layers (layers 2 and 3) were found to have the highest current (8.0×10^{-9} A) and this condition enhanced the high electrical conductivity of the solar cell.

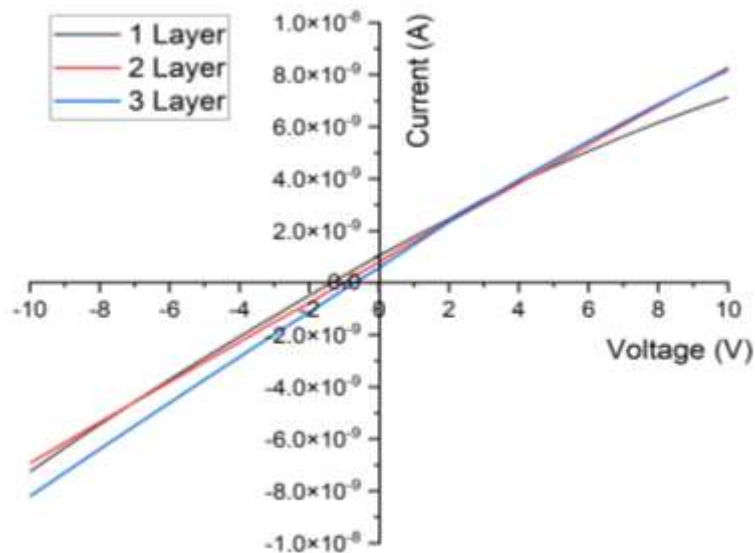


Fig. 5. I-V measurement plots of TiO₂ thin films with 3 different deposition layers.

Conclusion & Recommendation

This study has analysed the effects of the deposition layer of TiO₂ thickness on the performance of the dye-sensitized solar cell (DSSC) on the morphological, structural, optical, and electrical properties of the TiO₂ thin films. The results demonstrate that DSSC efficiency initially increases with the rise in TiO₂ film thickness because increasing the thickness improved the ability of the photoanode to absorb dye. The findings showed that when the thickness of the TiO₂ deposition layer increases, crystal quality increases. As film thickness increases, the crystals were observed to become bigger and the film surface becomes more compact and agglomerated.

In commercialisation perspective, DSSC can be concluded to be one of the photovoltaic cell which having a good potential for future commercialisation in indoor electricity application which is economically sustainable due to their advantages including abundant raw materials, a quick energy payback period, consistent power production and compatibility with flexible applications. Commercialisation of DSSC will accelerate the uptake of solar energy in both developed and developing nations. However, this can only be done if more research on the energy conversion effectiveness, long-term stability, and production cost being explored.

In conclusion, the commercialisation of DSSC technology has the potential to have a positive impact on the economy in a number of ways, including by lowering manufacturing costs, creating jobs opportunity, reducing cost of energy resources and increasing import-export opportunities. However, it also encounters obstacles with reliability, legal barriers, scalability of production and market competition. The extent to which these concerns are resolved and how successfully DSSC technology develops in the international solar industry will determine the total economic impact.

Acknowledgement

The authors would like to thank Ministry of Higher Education (MOHE) under grant FRGS/1/2021/TK0/UITM/02/12 for the financial support and Solar Research Institute (SRI), NANO-Electronic Centre, School of Electrical Engineering, School of Mechanical Engineering and Faculty of Applied Science of Universiti Teknologi MARA (UiTM) for facilities support.

References

- Kumavat, P. P., Sonar, P., & D. S. Dalal, D. S. (2017). An overview on basics of organic and dye sensitized solar cells, their mechanism and recent improvements. *Renewable & Sustainable Energy Reviews*, 78, 1262-1287. <https://doi.org/10.1016/j.rser.2017.05.011>.
- Liang, Y., Sun, S., Deng, T., Ding, H., Chen, W., & Chen, Y. (2018). The Preparation of TiO₂ Film by the Sol-Gel Method and Evaluation of Its Self-Cleaning Property. *Materials*, 11(3), 450. [Online]. <https://www.mdpi.com/1996-1944/11/3/450>.
- Richhariya, G., Kumar, A., Tekasakul, P., & Gupta, B. (2017). Natural dyes for dye sensitized solar cell: A review. *Renewable and Sustainable Energy Reviews*, 69, 705-718. <https://doi.org/10.1016/j.rser.2016.11.198>.
- Lal, M., Sharma, P., Ram, C. (2022). Synthesis and photocatalytic potential of Nd-doped TiO₂ under UV and solar light irradiation using a sol-gel ultrasonication method. *Results in Materials*, 15, 100308. <https://doi.org/10.1016/j.rinma.2022.100308>.
- Raguram, T., & Rajni, K. S. (2020). Influence of boron doping on the structural, spectral, optical and morphological properties of TiO₂ nanoparticles synthesized by sol-gel technique

- for DSSC applications. *Materials Today: Proceedings*, 33, 2110-2115. <https://doi.org/10.1016/j.matpr.2020.02.738>.
- Raguram, T., & Rajni, K. S. (2022). Synthesis and characterisation of Cu - Doped TiO₂ nanoparticles for DSSC and photocatalytic applications. *International Journal of Hydrogen Energy*, 47(7), 4674-4689. <https://doi.org/10.1016/j.ijhydene.2021.11.113>.
- Marien, C. B. D., Marchal, C., Koch, A., Robert, D., & Drogui, P. (2017). Sol-gel synthesis of TiO₂ nanoparticles: effect of Pluronic P123 on particle's morphology and photocatalytic degradation of paraquat. *Environmental Science and Pollution Research International*, 24(14), 12582-12588. <https://doi.org/10.1007/s11356-016-7681-2>.
- Soga, T. (2006). *Nanostructured Materials for Solar Energy Conversion*, Elsevier.
- Vinaayak, S. B., Balasubramani, V., Shkir, M., Manthrammel, M. A., & Sreedevi, G. (2022). Enhancing the performance of TiO₂ based N-DSSC using dye extracted from *Cladophora Columbiana*, *Ludwigia repens* and mixed sensitizer. *Optical Materials*, 133, 112968. <https://doi.org/10.1016/j.optmat.2022.112968>.
- Elsaedy, H. I., Qasem, A., Yakout, H. A., & Mahmoud, M. (2021). The pivotal role of TiO₂ layer thickness in optimizing the performance of TiO₂/P-Si solar cell. *Journal of Alloys and Compounds*, 867, 159150. <https://doi.org/10.1016/j.jallcom.2021.159150>.
- Castilhos, S., Souza, F., Colpini, L., Jorge, L., & Santos, O. (2020). Assessment comparison of commercial TiO₂ and TiO₂ sol-gel on the degradation of caffeine using artificial radiation, *Environmental Science and Pollution Research*, 27. <https://doi.org/10.1007/s11356-020-07748-x>.
- Low, K. T., Yam, F. K., Beh, K. P., Abd Manaf, A., & Beh, K. K. (2021). Characteristics and Sensing of Sol-gel derived Titanium Dioxide-based Ultraviolet Photodetector on Flame Retardant-4 Board," *Sensors and Actuators A: Physical*, vol. 323, p. 112654, 2021/06/01/2021, doi: <https://doi.org/10.1016/j.sna.2021.112654>.
- González-Verjan, V. A. *et al.* (2020). Effect of TiO₂ particle and pore size on DSSC efficiency. *Materials for Renewable and Sustainable Energy*, 9(2), 13. <https://doi.org/10.1007/s40243-020-00173-7>.
- Drygała, A. (2021). Influence of TiO₂ film thickness on photovoltaic properties of dye-sensitized solar cells. *IOP Conference Series: Earth and Environmental Science*, 642(1), 12001. <https://doi.org/10.1088/1755-1315/642/1/012001>.
- Morad, I., Alshehri, A. M., Mansour, A. F., Wasfy, M. H., & El-Desoky, M. M. (2020). Facile synthesis and comparative study for the optical performance of different TiO₂ phases doped PVA nanocomposite films. *Physica B: Condensed Matter*, 597, 412415. <https://doi.org/10.1016/j.physb.2020.412415>.
- Kao, M. C., Chen, H. Z., Young, S. L., Kung, C. Y., & Lin, C. C. (2009). The effects of the thickness of TiO₂ films on the performance of dye-sensitized solar cells. *Thin Solid Films*, 517(17), 5096-5099. <https://doi.org/10.1016/j.tsf.2009.03.102>.
- Ibrahim, S., & Sreekantan, S. (2010). Effect of pH on TiO₂ Nanoparticles via Sol-Gel Method. *Advanced Materials Research*, 173, 184-189. <https://doi.org/10.4028/www.scientific.net/AMR.173.184>.
- Faruk, H. M., Sarwar, P. M., & Nahid, M. A. I. (2020). Influence of film thickness on optical and morphological properties of TiO₂ thin films. *Emerging Materials Research*. 9(1), 186-191. <https://doi.org/10.1680/jemmr.17.00085>.
- Devi, P. K., Goswami, P., & Chaturvedi, H. (2022). Fabrication of nanocrystalline TiO₂ thin films using Sol-Gel spin coating technology and investigation of its structural, morphology

and optical characteristics. *Applied Surface Science*, 591, 153226.
<https://doi.org/10.1016/j.apsusc.2022.153226>.

Saad, M. P. S., Sutan, H., Shariffudin, S., Hashim, H., & Noor, M. U. (2006). TiO₂ Thin Film via Sol-Gel Method: Investigation on Molarity Effect. *IOP Conference Series: Materials Science and Engineering*, 99, 12006, <https://doi.org/10.1088/1757-899X/99/1/012006>.